Catalysis Communications 162 (2022) 106385

Contents lists available at ScienceDirect

Catalysis Communications

journal homepage: www.elsevier.com/locate/catcom

Short communication

Design of CO_2 hydrogenation catalysts based on phosphane/borane frustrated Lewis pairs and xanthene-derived scaffolds

Maicon Delarmelina [a,b,*], José Walkimar de M. Carneiro [c], C. Richard A. Catlow [a,b,d], Michael Bühl [e]

[a] School of Chemistry, Cardiff University, Main Building, Park Place, Cardiff CF10 3AT, UK
[b] UK Catalysis Hub, Research Complex at Harwell, STFC Rutherford Appleton Laboratory, Didcot, Oxfordshire OX11 0FA, UK
[c] Instituto de Química, Universidade Federal Fluminense, Niterói, Rio de Janeiro 24020-141, Brazil
[d] Department of Chemistry, University College London, 20 Gordon St, London WC1 HOAJ, UK
[e] School of Chemistry, University of St Andrews, North Haugh, St Andrews, KY16 9ST Fife, United Kingdom

ARTICLE INFO

Keywords:
Frustrated Lewis pair
Xanthene
CO_2 hydrogenation
Formic acid
DFT

ABSTRACT

New naphtho[2,1,8,7-klmn]xanthene and benzo[*kl*]xanthene-based intramolecular phosphane–borane frustrated Lewis pairs (FLPs) were investigated in catalyzed H_2 activation and CO_2 hydrogenation processes. According to DFT predictions at the B3LYP-D3 level, the presence of rigid scaffolds and increased P···B distances in the investigated FLPs lead to a remarkable drop in the energy barrier for CO_2 hydrogenation (by up to 19.2 kcal mol^{-1}, compared to the parent dimethylxanthene-based FLP). Furthermore, the energy differences between the transition states for H_2 activation and CO_2 hydrogenation are significantly reduced, making both processes feasible under relatively mild experimental conditions.

1. Introduction

The class of catalysts known as Frustrated Lewis Pairs (FLP) have received great attention since the first report by D·W Stephan *et al.* in 2006 [1]. In general, they are defined as Lewis acid-base pairs unable to form conventional Lewis adducts due to steric hindrance of their structure. A broader definition for FLP chemistry has also been commonly used [2]. The versatility of possible structures and their catalytic properties makes them potential candidates to replace metal-based catalysts in greener chemical processes [3,4]. Despite their promising catalytic properties, side-reactions and self-deactivation of these catalysts remain a great challenge to be overcome before large scale applications are possible. The key for higher efficiency and selectivity of FLPs lies in the identification of electronic and structural factors capable of fine tuning the reactivity and stability of these systems [5].

Amongst the most promising strategies for dealing with these challenges, the preparation of new intramolecular FLP systems supported by distinct backbones is an alternative for tailoring more efficient systems, beyond the conventionally investigated changes in steric repulsion and electronic effects of substituents. The pioneering work of Erker *et al.* has shown four-membered cyclic intramolecular phosphane–borane (P/B) adducts (vicinal FLPs, Fig. 1*i*) capable of catalyzing rapid H_2 splitting at room temperature and low H_2 pressure [6]. Other relevant examples of scaffolds for supporting FLPs are carbon atoms/chains as spacer (*e.g.* geminal [7] and vicinal [8] FLPs), phenylenes [9], naphthalenes [10], biphenylenes [11], dibenzofurans [12], macrocycles [13], and molecular cages [14], together with a range of modifications of distinct substituent groups that confer electron withdrawing/releasing effects onto the acid-base units of the resulting FLPs (Fig. 1*i*).

Recently, Mo and Aldridge [12] have shown how the use of the dimethylxanthene backbone to prevent intramolecular-type P/B interactions can lead to preorganized FLPs and tuned activity towards reversible activation of H_2 molecules (**1**, **Figure 1*ii***) [12]. As well as the structural effect, these authors also showed that with strongly donating alkyl-substituted phosphine components the hydrogenation reaction becomes irreversible (**2**, **Figure 1*ii***) [12] and that unsubstituted alkyl (phenyl) groups cause a reduction of the FLP activity (**3**, **Figure 1*ii***) [15]. On the other hand, the absence of electron withdrawing groups on B resulted in the quenching of the activity of these derivatives for H_2 splitting (**4**, **Figure 1*ii***) [15]. These derivatives were used in a wide range of applications, such as dihydrogenation of amine-boranes [15], C(sp)-H bond activation [16] and N_2O capture [12].

* Corresponding author at: School of Chemistry, Cardiff University, Main Building, Park Place, Cardiff CF10 3AT, UK.
E-mail address: delarmelinam@cardiff.ac.uk (M. Delarmelina).

https://doi.org/10.1016/j.catcom.2021.106385
Received 10 November 2021; Received in revised form 21 December 2021; Accepted 22 December 2021
Available online 24 December 2021

Motivated by the catalytic activity of xanthene-containing derivative **1a**, we have now applied density functional theory (DFT) to explore new xanthene-inspired scaffolds as backbones for intramolecular P/B FLPs, namely tribenzo[*b,d,f*]oxepine, naphtho[2,1,8,7-*klmn*]xanthene, and benzo[*kl*]xanthene (**Figure 1*iii***). Such structures were selected in order to probe how changes in the flexibility/rigidity of the linker bearing the Lewis acid and base units can affect the P···B interaction and, in particular, the reactivity towards H_2 activation and the subsequent CO_2 hydrogenation reaction to produce formic acid, which is a key step for the development of new catalysts for conversion of CO_2 into added-value chemicals, with potential applications in many industrial processes, from solvents and reactants production, to liquid fuel synthesis. [17] Generally, CO_2 hydrogenation has been thoroughly investigated in the context of heterogeneous catalysts [17]. Only recently examples of homogenous catalysts have been reported to be active for this reaction; however they are commonly formed by efficient, but expensive, noble metal complexes [18–20], or organic catalysts (including FLPs), which require harsh conditions, long reaction times, and/or lead to stoichiometric reactions [21–26]. In contrast, the new FLP systems proposed here prove to be potential candidates for applications in catalytic H_2 activation and CO_2 hydrogenation under relatively mild reaction conditions.

2. Results and discussion

Parent derivative **1a** was first analysed regarding its structure and reactivity. A key parameter commonly used in the rationalisation of the reactivity of FLPs is the interatomic distance between their acid and base units. As shown in Fig. 2a, 1a presents a P···B interatomic distance of $r_{B\ldots P} = 3.871$ Å. This distance is linked to the "hinge angle" at the central 4*H*-pyran moiety and can be modified through breathing (or wing-flapping) motion of the xanthene backbone. We assess this structural feature through the angle ϕ between the two aryl rings of the xanthene moiety, where $\phi = 180°$ implies perfect co-planarity (see Supporting Information for definition of ϕ). Interestingly, when acting as catalyst in H_2 activation, and consecutively in the CO_2 hydrogenation to produce formic acid (Fig. 2b), $r_{B\ldots P}$ and ϕ change significantly during binding or activation of the reactants, as is evident in the transition state structure

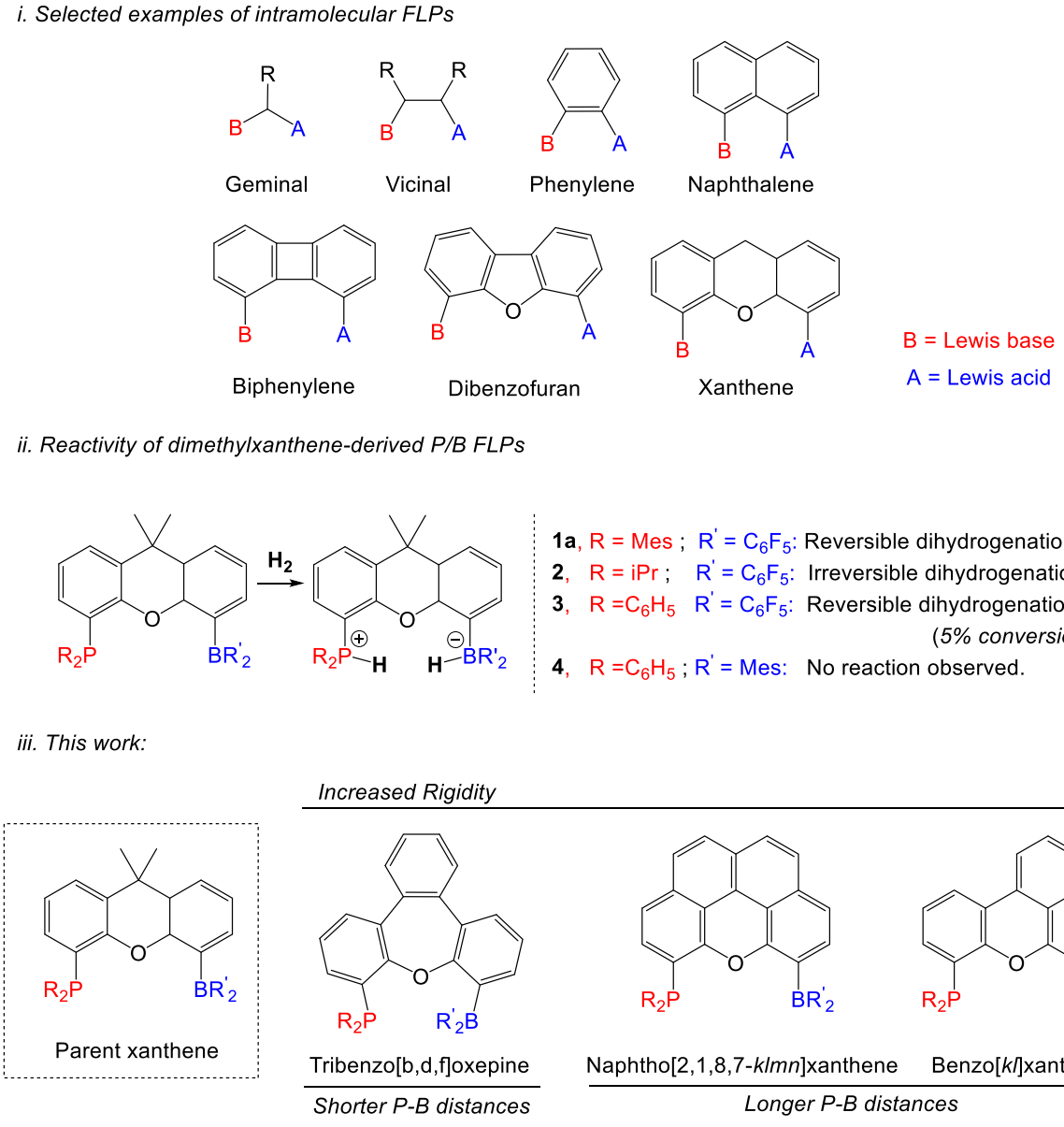

Fig. 1. (i) Commonly used scaffolds for the construction of intramolecular FLPs, (ii) previously reported reactivity of dimethylxanthene-based P/B FLPs in H_2 activation reaction, and (iii) proposed modifications of the xanthene-based backbone of P/B FLPs investigated in this work.

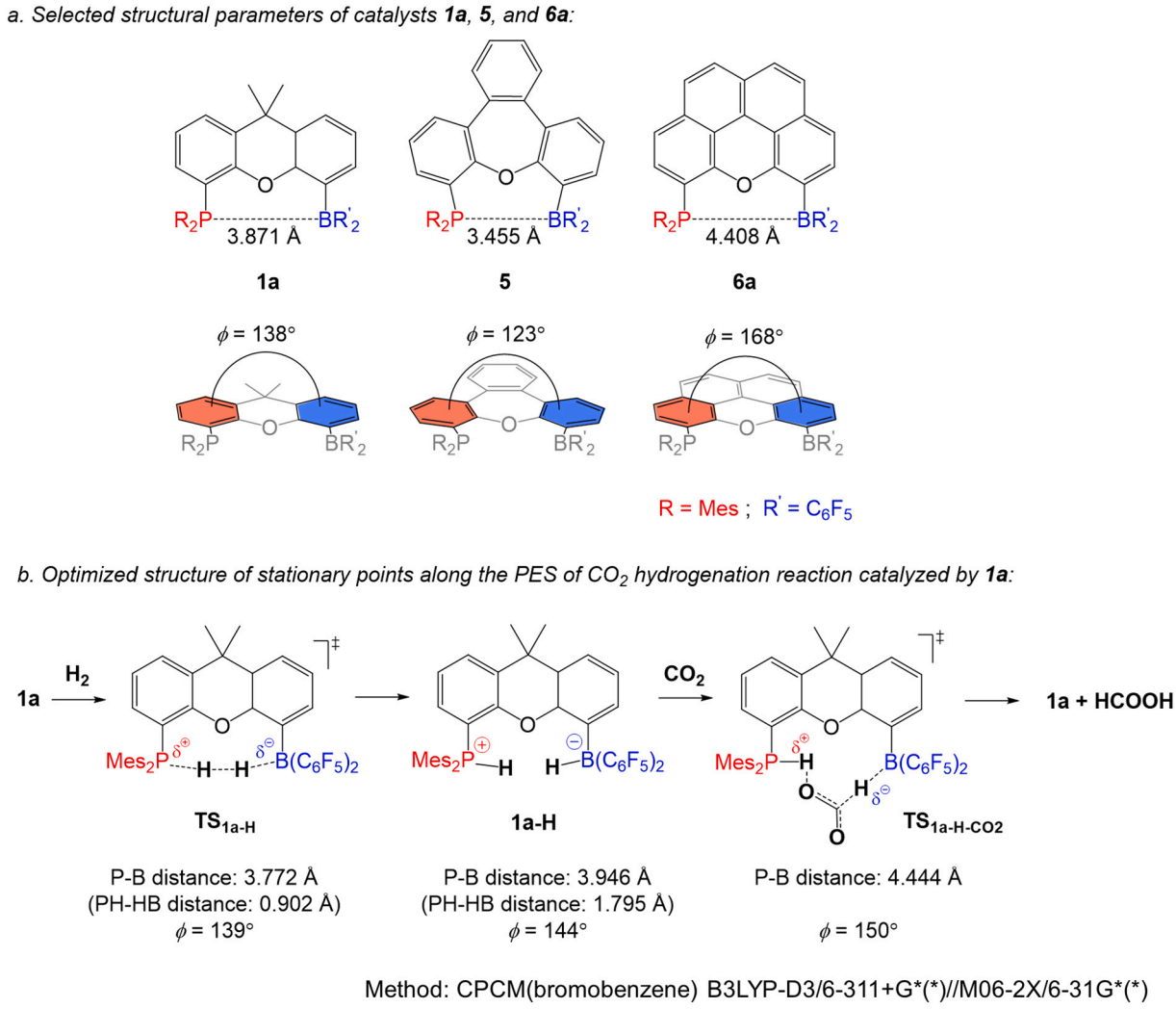

Fig. 2. (a) P···B interatomic distances (Å) and angles (degrees) between P- and B-containing aryl rings of derivatives **1a**, **5**, and **6a**, and (b) of derivative **1a** throughout the catalyzed CO_2 hydrogenation reaction. Angle between the aryl rings on the xanthene backbone was calculated according to the procedure described in subsection 2 of Supporting Information.

for the CO_2 hydrogenation step (**$TS_{1a\text{-}H\text{-}CO2}$**), in which $r_{B\ldots P}$ and ϕ increase by 0.573 Å and 12°, respectively, when compared to the isolated catalyst, **1a**. For the hydrogenation step (**$TS_{1a\text{-}H}$**), the structural changes of the dimethylxanthene backbone are less significant. However, it is still worth mentioning that the P···B distance is slightly reduced to facilitate the H—H bond cleavage (**$TS_{1a\text{-}H}$**, Fig. 2b).

The full energy profile for CO_2 hydrogenation catalyzed by **1a** is shown in Fig. 3. The calculated Gibbs free-energy barrier for H_2 activation is 11.6 kcal mol^{-1}, whereas the calculated barrier for the CO_2 hydrogenation step is 34.6 kcal mol^{-1}. Experimental studies showed that H_2 is readily activated by **1a** under mild reaction conditions - H_2 (1 atm), 22 °C, in C_6D_5Br, in agreement with the relative low energy barrier calculated here for such a process [12]. No experimental data are available regarding the CO_2 hydrogenation step catalyzed by **1a**. Nevertheless, the computed differences in the free energy barrier of 23.0 kcal mol^{-1} (an increase in enthalpy of 20.4 kcal mol^{-1}) compared to the previous step indicates that such process would not occur under similar experimental conditions. Similar high energy barriers for CO_2 hydrogenation have been reported for other classes of intramolecular P/B FLPs [27]. Finally, the computed reaction energy shows this to be an endothermic and endergonic process (ΔH_R = +2.1 kcal mol^{-1}, ΔG_R = +8.9 kcal mol^{-1}) in agreement with previous reports [28–30].

Based on the observations of shortening and increasing of the P···B interatomic distances observed for **1a** during H_2 activation and CO_2 hydrogenation processes, respectively, two new prototypic scaffolds were investigated: tribenzo[*b,d,f*]oxepine (**5**) and naphtho[2,1,8,7-*klmn*]xanthene (**6a**) backbones (Fig. 2). Both were constructed using mesitylene (−Mes) and pentafluorophenyl (-C_5F_6) substituents bonded to the P and B moieties, respectively, to allow direct comparison of their catalytic activity against that of the parent catalysts, **1a**. The optimized structures of **5** and **6a** have $r_{B\ldots P}$ = 3.445 Å and 4.408 Å, respectively. Effectively, these represent a shortening of the P···B distance by 0.416 Å for **5** and an increase by 0.537 Å for **6a**, when compared to **1a**. The angle between the aromatic rings holding the P and B units also changed significantly for these derivatives, with calculated values of 138°, 123°, and 168° for **1a**, **5**, and **6a**, respectively (Fig. 2). When these new FLPs were tested for their putative catalytic activity in H_2 activation (step 1, Fig. 3), both showed a slight increase in the calculated activation energy, in comparison to **1a** - an increase in the free energy barrier by +1.8 and + 4.0 kcal mol^{-1} for **5** and **6a**, respectively; even smaller if the enthalpies are calculated. In contrast, the subsequent energy barrier for the CO_2 hydrogenation step is significantly affected for the two FLPs, **5** and **6a**, as discussed next.

At this point, it is worth mentioning that in most cases investigated here, the calculated reaction energies for formation of the hydrogenated intermediate **X-H** showed this to be an exothermic and exergonic

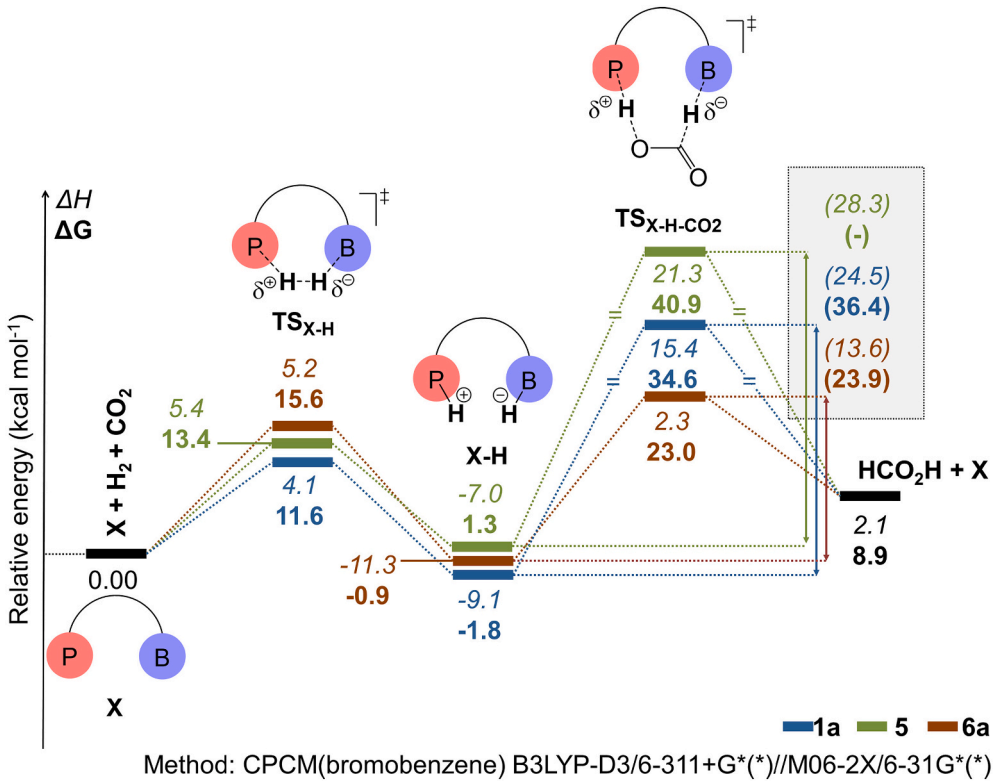

Fig. 3. Energy profile for H_2 activation and CO_2 hydrogenation catalyzed by the Frustrated Lewis Pairs **X** (**X** = **1a**, **5** and **6a**). Relative enthalpies (*italic*) and Gibbs free energy (**bold**) were calculated by taking the isolated reactants as reference. Energy differences between points **X-H** and $\mathbf{TS_{X\text{-}H\text{-}CO2}}$ are given in parenthesis for the cases in which this is the rate-determining step.

process (*e.g.* **1a-H** and **6a-H**, Fig. 3). For these cases, intermediate **X-H** is the resting stage of the catalytic mechanism; thus it should be considered in the calculation of the energy barrier for the CO_2 hydrogenation step, in accordance with the Energy Span Model conceptualised by Kozuch and Shaik [31,32]. Accordingly, the energy difference between points **X-H** and $\mathbf{TS_{X\text{-}H\text{-}CO2}}$ are also given in Fig. 3. For **5**, however, formation of **X-H** was computed as a slightly endergonic process, although the enthalpy change still showed this to be exothermic (*e.g.* **5-H**, Fig. 3). In this case, the resting state on the catalytic cycle is that with the isolated reactants, and the free energy barrier for CO_2 hydrogenation step is the same as the relative energy of the corresponding transition state structure $\mathbf{TS_{X\text{-}H\text{-}CO2}}$; when comparing enthalpies, the energy difference between points **X-H** and $\mathbf{TS_{X\text{-}H\text{-}CO2}}$ should still be considered. For predictions concerning the energy span under turnover conditions, the endothermicity and endergonicity of the overall catalytic process also need to be taken into consideration, *i.e.* the energy span under turnover conditions is determined by the energy barrier for the CO_2 hydrogenation step, as discussed above, summed to the calculated reaction energy variations ($\Delta H_R = +2.1$ kcal mol^{-1} and $\Delta G_R = +8.9$ kcal mol^{-1}, Fig. 3). Nevertheless, as the latter remains unaltered for all investigated systems, the comparison of the changes in the energy barrier for individual steps of the catalytic process suffice to rationalise the catalytic activities studied here. Later on, the same approach will be used for the results presented in Table 1.

Taking into consideration the points discussed above, while the CO_2 hydrogenation step catalyzed by **5** led to a + 4.5 kcal mol^{-1} increase in the calculated activation free energy (+3.8 kcal mol^{-1} for enthalpy, Fig. 3), catalyst **6a** led to a notable reduction of −12.5 kcal mol^{-1} in the activation free energy (−10.9 kcal mol^{-1} for enthalpy, Fig. 3). Therefore, while the large P···B distance in **6a** and the rigid nature of its backbone structure led to an increase in the activation energy for step 1, in contrast, such features led to substantial reduction in the activation energy for step 2. As the activation energy for step 2 is higher than that for step1, which itself is relatively low, the general effect is a reduction in the activation energy for the whole process. In addition, we considered possible effects from using solvents with different polarities for selected FLPs. Repeating the single-point energy calculations in the gas phase (as ultimate limit for nonpolar solvents) and in a continuum using the parameters of DMSO (a highly polar solvent) raises and lowers, respectively, the relative energies of both intermediate **X-H** and transition state $\mathbf{TS_{X\text{-}H\text{-}CO2}}$ when the energy of the isolated reactants are taken as reference. However, for both the key difference is affected only to a small extent (up to 2.6 kcal mol^{-1}, see **Table S2**, Supporting Information).

Next, we explored modifications in substituents R and R' in **1a** and **6a**, in an attempt to achieve further reduction in the activation energy for the CO_2 hydrogenation step. The effects of electron-withdrawing or electron-releasing groups were evaluated by two approaches: (i) by replacing the pentafluorophenyl (-C_6F_5) group by a 3,5-bis(trifluoromethyl)phenyl (-Ph$(CF_3)_2$) substituent at the B moiety, reducing the Lewis acidity of the borane; (ii) by replacing the mesitylene (−Mes) group by a 1,3-diisopropyl-5-methyl-phenyl (-DIMP) substituent at the P moiety, to verify the electron-donating effects of alkyl substituents on the basicity of the phosphane. Although an extensive list of potential modifications to FLPs could be proposed based on previous experimental and computational studies, [3–5] the resulting electronic effects reported before are similar to the ones investigated here. Furthermore, when compared to the distinct FLP backbones investigated here, changes in the electron realising/withdrawing abilities of substituents groups are expected to have a less significant effect over the calculated energy barriers, as will be discussed next.

The calculated energy data for these new FLP catalysts is given in Table 1. The calculated free energy barrier for H_2 activation catalyzed by dimethylxanthene-based FLPs (**1a-1d**, Table 1) ranged from 11.6 to 16.5 kcal mol^{-1} (from 3.9 to 6.7 kcal mol^{-1} if enthalpy is considered). The lowest barrier for this step is observed for **1a**, whereas **1c** has the

Table 1
Relative energy for H_2 activation and CO_2 hydrogenation catalyzed by **X** (a, **X** = **1a**, **1b**, **1c**, and **1d**; b, **X** = **6a**, **6b**, **6c** and **6d;** c, **X** = **7** and **8**). The relative energies (kcal mol^{-1}) were calculated by taking the energy of the isolated reactants as reference. Values in parentheses are the relative energies between points **X-H** and $\mathbf{TS_{X\text{-}H\text{-}CO2}}$ ($\mathbf{\Delta\Delta E\ (X\text{-}H,\ TS_{X\text{-}H\text{-}CO2})}$) for the cases in which this is the rate-determining step.

a. Dimethylxanthene-based P/B FLPs

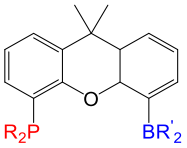

	R	R'		$TS_{X\text{-}H}$	X-H	$TS_{X\text{-}H\text{-}CO2}$	$\Delta\Delta E$ (X-H, $TS_{X\text{-}H\text{-}CO2}$)
1a	Mes	C_5F_6	*ΔH*	*4.1*	*−9.1*	*15.4*	*−24.5*
			ΔG	11.6	−1.8	34.6	−36.4
1b	DIMP	C_5F_6	*ΔH*	*3.9*	*−10.6*	*9.8*	*−20.4*
			ΔG	13.9	−1.6	32.5	−34.1
1c	Mes	$Ph(CF_3)_2$	*ΔH*	*6.7*	*−4.0*	*14.9*	*−18.9*
			ΔG	16.5	2.1	35.1	(–)
1d	DIMP	$Ph(CF_3)_2$	*ΔH*	*4.5*	*−4.9*	*18.4*	*−23.3*
			ΔG	13.2	3.6	39.0	(–)

b. Naphtho[2,1,8,7-klmn]xanthene-based P/B FLPs

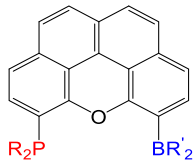

	R	R'		$TS_{X\text{-}H}$	X-H	$TS_{X\text{-}H\text{-}CO2}$	$\Delta\Delta E$ (X-H, $TS_{X\text{-}H\text{-}CO2}$)
6a	Mes	C_5F_6	*ΔH*	*5.2*	*−11.3*	*2.3*	*−13.6*
			ΔG	15.6	−0.9	23.0	−23.9
6b	DIMP	C_5F_6	*ΔH*	*6.7*	*−13.4*	*−0.3*	*−13.1*
			ΔG	16.2	−3.6	21.4	−25.0
6c	Mes	$Ph(CF_3)_2$	*ΔH*	*7.7*	*−3.0*	*3.1*	*−6.1*
			ΔG	15.0	3.1	23.0	(–)
6d	DIMP	$Ph(CF_3)_2$	*ΔH*	*6.8*	*−11.1*	*0.2*	*−11.3*
			ΔG	13.5	3.8	17.2	(–)

c. Benzo[kl]xanthene-based P/B FLPs

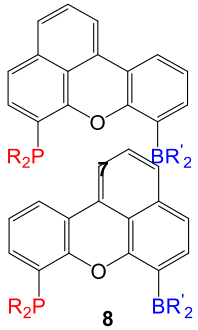

	R	R'		$TS_{X\text{-}H}$	X-H	$TS_{X\text{-}H\text{-}CO2}$	$\Delta\Delta E$ (X-H, $TS_{X\text{-}H\text{-}CO2}$)
7	DIMP	$Ph(CF_3)_2$	*ΔH*	*6.8*	*−11.5*	*2.7*	*−14.2*
			ΔG	16.3	−1.6	22.2	−23.8
	R	**R'**		$TS_{X\text{-}H}$	**X-H**	$TS_{X\text{-}H\text{-}CO2}$	$\Delta\Delta E$ (X-H, $TS_{X\text{-}H\text{-}CO2}$)
8	DIMP	$Ph(CF_3)_2$	*ΔH*	*6.0*	*−9.5*	*2.4*	*−11.9*
			ΔG	14.6	0.1	22.4	(–)

Method: CPCM(bromobenzene) B3LYP-D3/6–311+G*(*)//M06-2X/6-31G*(*)

highest enthalpy and free energy barrier in the set. Conversely, **1a** and **1c** led to the highest (24.5 kcal mol^{-1}) and the lowest (18.9 kcal mol^{-1}) activation enthalpy for the CO_2 hydrogenation step, respectively.

Similar energy ranges were observed for naphtho[2,1,8,7-klmn] xanthene-based FLPs (**6a-6d**, Table 1). The derivative bearing the -Mes and -$Ph(CF_3)_2$ substituents (**6c**) was calculated to have the lowest activation enthalpy for CO_2 hydrogenation (6.1 kcal mol^{-1}) at the expense of a slight increase in the activation enthalpy for H_2 activation (7.7 kcal mol^{-1}). Remarkably, **6c** has an enthalpy profile in which the rate determining step is the H_2 activation and not the CO_2 hydrogenation step. When free energies are considered, derivative **6d** presented the lowest barriers, 13.5 kcal mol^{-1} for step 1 and 17.2 kcal mol^{-1} for step 2.

In order to verify the effect of the rigidity of derivatives **6a-6d** on the activation energy for CO_2 hydrogenation, two additional FLP models were designed by using a benzo[*kl*]xanthene backbone: derivatives **7** and **8** (Table 1), both bearing -DIMP and -$Ph(CF_3)_2$ substituents. The absence of one fused benzene ring in their structure resulted in a slight increase in the free energy barrier for H_2 activation (by 3.0 and 1.1 kcal mol^{-1} for **7** and **8**, respectively) when compared to **6d**. On the other hand, a more significant change was observed in the free energy barrier of the CO_2 hydrogenation step, which increased by 6.6 and 5.2 kcal mol^{-1} for **7** and **8**, respectively. Still, these energy barriers are significantly smaller than those obtained for the parent FLP **1a**.

Finally, it should be noted that catalysts for CO_2 hydrogenation should also be potent catalysts for the reverse reaction, *i.e.,* dehydrogenation of formic acid. In fact, for complex **6d,** the barrier for this process (forming **6d-H** under liberation of CO_2) is computed to be just 8.3 kcal mol^{-1}, that for H_2 release to regenerate **6d** is only slightly higher, 9.8 kcal mol^{-1} (see data in Table 1). Ruthenium-based complexes have been developed for this purpose, with potential use in powering fuel cells with H_2 produced from formic acid as fuel [33,34]. In the spirit of the 2021 Nobel prize in chemistry for organocatalysis [35], FLPs of the type we have identified could be greener and cheaper alternatives to these toxic and expensive heavy-metal catalysts. An additional advantage of FLPs in practical applications could be that once immobilized through covalent attachment to a solid support, catalyst recovery should be easy, without any danger of metal leaching.

3. Conclusions

For the intramolecular P/B FLPs containing the rigid naphtho [2,1,8,7-klmn]xanthene and benzo[*kl*]xanthene backbones, we predict a remarkable reduction in the activation energy for CO_2 hydrogenation, at the expense of slight increase in the preliminary H_2 activation step, compared to the parent dimethylxanthene-based FLP **1a**. For the new FLPs designed in this work, the lowest calculated free energy barrier for CO_2 hydrogenation is 17.2 kcal mol^{-1} (*ca.* 26 kcal mol^{-1} under turnover). These are, to the best of our knowledge, the first examples of xanthene-inspired intramolecular P/B FLPs with potential to allow

kinetically accessible H_2 activation and subsequent CO_2 hydrogenation processes under relatively mild reaction conditions. These FLPs are also predicted to be promising candidates for catalyzing the reverse process, namely H_2 release from formic acid.

Declaration of competing interest

There are no conflicts to declare.

Acknowledgements

The authors dedicate this publication to the memory of Prof Paul Kamer and his work on the chemistry of XantPhos which inspired this investigation. UK Catalysis Hub is kindly thanked for resources and support provided *via* our membership of the UK Catalysis Hub Consortium and funded by EPSRC grant: EP/R026939/1, EP/R026815/1, EP/R026645/1, EP/R027129/1, and EP/M013219/1. J.W.M.C. acknowledges financial support from FAPERJ (grants E-26/203.001/2017, E-26/010.101118/2018, and E-26010.001424/2019) and CNPq (grants 309080/2015-0 and 434955/2018-3). M.B. thanks the School of Chemistry in St Andrews and EaStCHEM for support.

Appendix A. Supplementary data

Supplementary data to this article can be found online at https://doi.org/10.1016/j.catcom.2021.106385.

References

[1] G.C. Welch, R.R.S. Juan, J.D. Masuda, D.W. Stephan, Reversible, metal-free hydrogen activation, Science (80-.). 314 (2006) 1124–1126.
[2] D.W. Stephan, The broadening reach of frustrated Lewis pair chemistry, Science 80 354 (2016).
[3] G. Fiorani, W. Guo, A.W. Kleij, Sustainable conversion of carbon dioxide: the advent of organocatalysis, Green Chem. 17 (2015) 1375–1389.
[4] D.W. Stephan, Frustrated Lewis pairs: from concept to catalysis, Acc. Chem. Res. 48 (2015) 306–316.
[5] F.G. Fontaine, É. Rochette, Ambiphilic molecules: from organometallic curiosity to metal-free catalysts, Acc. Chem. Res. 51 (2018) 454–464.
[6] P. Spies, et al., Rapid intramolecular heterolytic dihydrogen activation by a four-membered heterocyclic phosphane–borane adduct, Chem. Commun. 2 (2007) 5072.
[7] C. Appelt, et al., Geminal phosphorus/aluminum-based frustrated Lewis pairs: C—H versus C—C activation and CO 2 fixation, Angew. Chem. Int. Ed. 50 (2011) 3925–3928.
[8] M. Sajid, et al., Noninteracting, vicinal frustrated P/B-Lewis pair at the Norbornane framework: synthesis, characterization, and reactions, J. Am. Chem. Soc. 135 (2013) 8882–8895.
[9] K. Chernichenko, M. Nieger, M. Leskelä, T. Repo, Hydrogen activation by 2-boryl-N,N-dialkylanilines: A revision of Piers' ansa-aminoborane, Dalton Trans. 41 (2012) 9029–9032.
[10] S. Bontemps, et al., Phosphino-boryl-naphthalenes: geometrically enforced, yet Lewis acid responsive P → B interactions, Inorg. Chem. 52 (2013) 4714–4720.
[11] F. Kutter, E. Lork, J. Beckmann, Frustrated Lewis pair based on a peri -substituted Biphenylene scaffold, Z. Anorg. Allg. Chem. 644 (2018) 1234–1237.
[12] Z. Mo, et al., Facile reversibility by design: tuning small molecule capture and activation by single component frustrated Lewis pairs, J. Am. Chem. Soc. 137 (2015) 12227–12230.
[13] L. Wang, et al., Formation of macrocyclic ring systems by carbonylation of trifunctional P/B/B frustrated Lewis pairs, Chem. Sci. 9 (2018) 1544–1550.
[14] J. Yang, et al., Endohedral functionalized cage as a tool to create frustrated Lewis pairs, Angew. Chem. Int. Ed. 57 (2018) 14212–14215.
[15] Z. Mo, A. Rit, J. Campos, E.L. Kolychev, S. Aldridge, Catalytic B-N dehydrogenation using frustrated Lewis pairs: evidence for a chain-growth coupling mechanism, J. Am. Chem. Soc. 138 (2016) 3306–3309.
[16] P. Vasko, et al., Reversible C−H activation, facile C−B/B−H metathesis and apparent hydroboration catalysis by a dimethylxanthene-based frustrated Lewis pair, Chem. - A Eur. J. 24 (2018) 10531–10540.
[17] X. Jiang, X. Nie, X. Guo, C. Song, J.G. Chen, Recent advances in carbon dioxide hydrogenation to methanol via heterogeneous catalysis, Chem. Rev. 120 (2020) 7984–8034.
[18] J. Kothandaraman, A. Goeppert, M. Czaun, G.A. Olah, G.K.S. Prakash, Conversion of CO 2 from air into methanol using a polyamine and a homogeneous ruthenium catalyst, J. Am. Chem. Soc. 138 (2016) 778–781.
[19] S. Wesselbaum, T. vom Stein, J. Klankermayer, W. Leitner, Hydrogenation of carbon dioxide to methanol by using a homogeneous ruthenium-phosphine catalyst, Angew. Chem. Int. Ed. 51 (2012) 7499–7502.
[20] C.A. Huff, M.S. Sanford, Cascade catalysis for the homogeneous hydrogenation of CO_2 to methanol, J. Am. Chem. Soc. 133 (2011) 18122–18125.
[21] A.E. Ashley, A.L. Thompson, D. O'Hare, Non-metal-mediated homogeneous hydrogénation of CO2 to CH3OH, Angew. Chem. Int. Ed. 48 (2009) 9839–9843.
[22] S.D. Tran, T.A. Tronic, W. Kaminsky, D. Michael Heinekey, J.M. Mayer, Metal-free carbon dioxide reduction and acidic C–H activations using a frustrated Lewis pair, Inorg. Chim. Acta 369 (2011) 126–132.
[23] T. Voss, et al., Frustrated Lewis Pair behavior of intermolecular amine/B(C 6 F 5) 3 Pairs, Organometallics 31 (2012) 2367–2378.
[24] M.-A. Courtemanche, et al., Intramolecular B/N frustrated Lewis pairs and the hydrogenation of carbon dioxide, Chem. Commun. 51 (2015) 9797–9800.
[25] L. Liu, N. Vankova, T. Heine, A kinetic study on the reduction of CO 2 by frustrated Lewis pairs: from understanding to rational design, Phys. Chem. Chem. Phys. 18 (2016) 3567–3574.
[26] T. Zhao, X. Hu, Y. Wu, Z. Zhang, Hydrogenation of CO 2 to formate with H 2 : transition metal free catalyst based on a lewis pair, Angew. Chem. Int. Ed. 58 (2019) 722–726.
[27] B. Jiang, Q. Zhang, L. Dang, Theoretical studies on bridged frustrated Lewis pair (FLP) mediated H2 activation and CO2 hydrogenation, Org. Chem. Front. 5 (2018) 1905–1915.
[28] K. Tedsree, et al., Hydrogen production from formic acid decomposition at room temperature using a ag–Pd core–shell nanocatalyst, Nat. Nanotechnol. 6 (2011) 302–307.
[29] H. Reymond, J.J. Corral-Pérez, A. Urakawa, P. Rudolf von Rohr, Towards a continuous formic acid synthesis: a two-step carbon dioxide hydrogenation in flow, React. Chem. Eng. 3 (2018) 912–919.
[30] A. Álvarez, et al., Challenges in the greener production of formates/formic acid, methanol, and DME by heterogeneously catalyzed CO 2 hydrogenation processes, Chem. Rev. 117 (2017) 9804–9838.
[31] S. Kozuch, S. Shaik, A combined kinetic-quantum mechanical model for assessment of catalytic cycles: application to cross-coupling and heck reactions, J. Am. Chem. Soc. 128 (2006) 3355–3365.
[32] S. Kozuch, S. Shaik, How to conceptualize catalytic cycles? The energetic span model, Acc. Chem. Res. 44 (2011) 101–110.
[33] M. Nielsen, et al., Low-temperature aqueous-phase methanol dehydrogenation to hydrogen and carbon dioxide, Nature 495 (2013) 85–89.
[34] D. Mellmann, P. Sponholz, H. Junge, M. Beller, Formic acid as a hydrogen storage material – development of homogeneous catalysts for selective hydrogen release, Chem. Soc. Rev. 45 (2016) 3954–3988.
[35] O. Shimomura, M. Chalfie, R.Y. Tsien, The nobel prize in chemistry, in: Nobel Lectures: Chemistry: 2006–2010, 2014, pp. 73–74.